is assigned to a $\pi'-\pi'^*$ transition. In order to ascertain existences of $\pi'-\pi'^*$ transitions in other diphenylpolyynes (C_6H_5—(C≡C)$_n$—C_6H_5, $n = 1 \sim 8$), modified PPP calculations are performed, and the results are shown in Table IV together with the experimental ones.[10] The calculated first and second transition energies decrease with increasing n. The intensity of the first transition decreases slightly with increasing n, while that of the second one increases remarkably.[4] These calculated results accord perfectly with the experimental ones obtained by Armitage et al.[10] The first electronic band of each compound is due to a $\pi-\pi^*$ transition and the second one to a $\pi'-\pi'^*$ transition.

IV. Conclusion

Diphenylpolyynes have two kinds of π electronic systems, π and π', which are mutually perpendicular. Therefore, the polyynes may show $\pi'-\pi'^*$ bands other than ordinarily observed $\pi-\pi^*$ bands. The 38 020-cm^{-1} band of diphenylbutadiyne has been assigned to a $\pi'-\pi'^*$ transition from its location, intensity, polarization, and temperature dependence of the band intensity. The 38 020-cm^{-1} band behaves in opposition to the Shpol'skii effect; i.e., the intensity of the band decreases with decreasing temperature, while that of the 30 250-cm^{-1} band, which is assigned to the first $\pi-\pi^*$ transition, increases. We may explain the above experimental facts by considering a weak interaction between the π' (and σ) electronic system of diphenylbutadiyne and the σ electronic system of the polymer molecule. That is, in this system the guest molecule combines with the host one in such a manner that the π electronic system cannot interact with the σ framework of the host molecule. As a result, the π electronic system of the guest molecule behaves as that of an isolated gas molecule. This might be an explanation for the reason of the Shpol'skii effect. In order to ensure the above explanation for the Shpol'skii effect, it is necessary to accumulate experimental data about compounds having two kinds of π electronic systems, π and π'. Furthermore, in the present MO calculations, the interaction between π' and σ electronic systems in diphenylbutadiyne was neglected, but it might be necessary to take account of the effect of it in the MO calculations.

Registry No. Diphenylbutadiyne, 886-66-8.

Gas-Phase Reactivity of the HCO Radical with Unsaturated Hydrocarbons: An Experimental and Theoretical Study

R. Lesclaux,*‡ P. Roussel,‡ B. Veyret,‡ and C. Pouchan†

Contribution from UA 348 CNRS, Laboratoire de Chimie Physique A, Université de Bordeaux I, 33405 Talence, France, and UA 474 CNRS, Laboratoire de Chimie Structurale, Université de Pau, 64000 Pau, France. *Received October 9, 1985*

Abstract: The kinetics and mechanism of the reactions of HCO radicals with a series of unsaturated hydrocarbons were studied experimentally by the flash photolysis-laser resonance absorption technique and theoretically, in the particular case of ethylene, by ab initio SCF MO calculations with double ζ basis sets. Experiments were carried out in the temperature range 350–510 K by photolyzing acetaldehyde for the generation of HCO. The Arrhenius expressions obtained are the following, in cm^3·molecule^{-1}·s^{-1} units: ethylene, $(1.5 \pm 0.6) \times 10^{-13} \exp[-(2750 \pm 75\ K/T)]$; propene, $(1.7 \pm 0.9) \times 10^{-13} \exp[-(2700 \pm 100\ K/T)]$; isobutene, $(5.45 \pm 2.9) \times 10^{-13}$, $\exp[-(3125 \pm 130\ K/T)]$; 1-butene, $(3.8 \pm 2.7) \times 10^{-13} \exp[-(3000 \pm 180\ K/T)]$; 2-butene, $(3.3 \pm 2.8) \times 10^{-13} \exp[-(3000 \pm 220\ K/T)]$; and 1,3-butadiene, $(5.8 \pm 1.3) \times 10^{-13} \exp[-(2050 \pm 50\ K/T)]$. The uncertainties quoted are equal to 2σ. The reactivity of the HCO radical with respect to that of unsaturated hydrocarbons is compared to that of other radicals. The end-product analysis in the photolysis of the acetaldehyde–olefin (or butadiene) system has shown that the reaction essentially proceeds via an addition mechanism, rather than a hydrogen atom transfer from HCO to the double bond, which is also energetically favorable. This is the first characterized reaction of HCO which does not involve such a hydrogen transfer from the radical. These results are supported by quantum mechanical calculations of the potential energy surfaces involved in the two possible reaction channels. These calculations show in particular that the energy barrier is much higher for the hydrogen atom transfer channel than for the addition process. In addition, calculated activation energies and preexponential factors are in good agreement with experimental results.

The formyl radical is an important intermediate in the chemistry and photochemistry of aldehydes in the gas phase and in oxidizing systems involving hydrocarbons. However, little is known to date concerning its reactivity. The main reaction of HCO in the oxidation of hydrocarbons, either in combustion or in atmospheric processes, is the fast reaction with molecular oxygen yielding CO and the HO_2 radical. The rate constant for this reaction, along with that for the similar reaction of HCO with NO, has been measured by several authors.[1]

$$HCO + O_2 \rightarrow CO + HO_2 \qquad \Delta H = -32\ \text{kcal·mol}^{-1} \quad (1)$$

$$HCO + NO \rightarrow CO + HNO \qquad \Delta H = -33\ \text{kcal·mol}^{-1} \quad (2)$$

$k_1 = 5.5 \times 10^{-12}$,

$k_2 = 1.2 \times 10^{-11}$ cm^3·molecule^{-1}·s^{-1} at 298 K

In the absence of oxygen (in the photochemistry of aldehydes for example) HCO reacts essentially with itself or with other radicals (H, CH_3, ...).

$$HCO + HCO \rightarrow CO + HCHO \qquad \Delta H = -70\ \text{kcal·mol}^{-1} \quad (3)$$

$$HCO + H \rightarrow CO + H_2 \qquad \Delta H = -87\ \text{kcal·mol}^{-1} \quad (4)$$

$$HCO + CH_3 \rightarrow CO + CH_4 \qquad \Delta H = -87\ \text{kcal·mol}^{-1} \quad (5)$$

All these reactions are fast: $k = 3\text{–}11 \times 10^{-11}$ cm^3·molecule^{-1}·s^{-1} at room temperature.

Hydrogen abstraction by the HCO radical from molecules is highly unlikely because of the relatively weak C–H bond formed in formaldehyde: D(H–CHO) = 87 kcal·mol^{-1}. Most hydrogen

† Université de Pau.
‡ Université de Bordeaux I.

(1) Temps, F.; Wagner, H. Gg. *Ber. Bunsen-Ges. Phys. Chem.* **1984**, *88*, 410. Langford, A. O; Moore, C. B. *J. Chem. Phys.* **1984**, *80*, 4211 and references therein.

0002-7863/86/1508-3872$01.50/0

abstraction reactions would be endothermic or would exhibit significant activation energies. They could be efficient only at high temperatures but at these temperatures HCO preferentially decomposes into H + CO since the C–H bond energy is very low.

$$HCO \rightarrow CO + H \qquad \Delta H = 17 \text{ kcal·mol}^{-1} \qquad (6)$$

Reactions 1–6 are the only HCO reactions for which kinetic data are available to describe the reactivity of this radical. It is interesting to point out that all these reactions proceed by hydrogen transfer from HCO to the reactant, and, therefore, the question arises as to the possibility of HCO reacting via a different elementary mechanism.

The main reaction channel of a radical species with an olefin is the addition to the double bond. The HCO radical may react in that way or via a hydrogen transfer. Both channels are energetically possible. For example, in the particular case of ethylene, the reactions are the following:

$$HCO + C_2H_4 \rightarrow CH_2CH_2CHO \qquad \Delta H = -19\text{kcal·mol}^{-1} \qquad (7a)$$

$$HCO + C_2H_4 \rightarrow CO + C_2H_5 \qquad \Delta H = -21 \text{ kcal·mol}^{-1} \qquad (7b)$$

Both reactions are of interest since reaction 7a does not involve the transfer of the hydrogen atom from HCO while reaction 7b is an original case in which the addition to the olefinic double bond occurs according to a hydrogen atom transfer mechanism.

No information is available concerning the reactivity of HCO with unsaturated hydrocarbons apart from the study of the reaction with 1,3-butadiene[2] that was performed in this laboratory, within the scope of the present work. This reaction is fairly efficient, particularly at temperatures higher than 400 K: $k(HCO + 1,3\text{-}C_4H_6) = 5.8 \times 10^{-13} \exp(-2070/T)$ cm^3·molecule^{-1}·s^{-1}, and proceeds according to an addition mechanism.

The reactions of HCO with unsaturated hydrocarbons are not only important for the general knowledge of the HCO chemistry but they can also be involved in the particular condition of weakly oxidizing systems, in spite of the fast reaction of HCO with O_2. For example, Moortgat et al.[3] have envisaged the occurrence of the reaction of HCO with propene to account for their results for the photolysis of the formaldehyde–propene system. However, their assumption could not be supported by any kinetic data.

In this paper, we report an experimental and theoretical study of the kinetics and reaction pathway for the reactions of HCO with a series of olefins.

The rate constant parameters were measured experimentally by flash photolysis, using laser resonance absorption for the detection of HCO. The Arrhenius parameters were determined for ethylene, propene, isobutene, 1-butene, and 2-butene in the temperature range 350–520 K. The reactions are slow and therefore measurements had to be performed at olefin pressures higher than 200 torr. The reaction channel was determined in the case of isobutene by end product analysis in the continuous photolysis of acetaldehyde–isobutene mixtures.

The experimental results were supported and interpreted by a theoretical analysis of reactions 7a and 7b in the anticipation that the system may be representative of HCO reactions with more complex olefins. Our primary purpose was to gain, from a quantum mechanical point of view, some knowledge of the potential surfaces, especially reaction barriers and geometries for the transition states in the two mechanisms. This information about the potential energy curves of the interacting constituents is necessary in order to obtain structural, spectroscopic, thermodynamic, and kinetic data. All computations were performed within the framework of ab initio Hartree–Fock SCF theory.

The purpose of such computations was not to achieve a complete description of this relatively complicated system but rather to help understand the experimental results by providing an additional insight into the reaction mechanism.

Experimental Section

HCO radicals were produced by flash photolysis of acetaldehyde, by using conventional flash lamps filled with argon. At the high pressures used in this study (300–700 torr), the radicals are thermalized more rapidly than the subsequent decay due to the reaction with the scavenger.

The flash photolysis-laser resonance absorption apparatus, adapted to the study of HCO reaction kinetics, has already been described,[4] and only the principal features are mentioned here. The reaction cell is a Pyrex cylinder, 70 cm long and 6 cm in diameter, fitted with two antireflective coated windows. Two cylindrical flash lamps are mounted parallel to the cell and deliver 100–400 J per pulse in less than 5 μs.

The radical concentration is monitored continuously by using a CW dye laser (Spectra Physics 580), tuned to the head of the HCO absorption band at 614.5 nm (0,9,0 ← 0,0,0 vibrational band). The absorption cross section at this wavelength was measured in a previous work: $\sigma = 1.07 \times 10^{-18}$ cm^2 ($\epsilon = 280$ M^{-1}·cm^{-1}) for a laser line width of 0.25 A.[5] No significant pressure dependence of σ could be detected, probably due to the strong overlap of the rotational lines in this region. However, σ slightly decreases with temperature,[5] and the HCO quantum yield is significantly reduced at high pressure. The flash energy therefore had to be raised as the temperature and pressure increased. The HCO concentrations used in experiments ranged from $1–5 \times 10^{13}$ molecule·cm^{-3}.

The HCO decay curves were averaged and stored in a multichannel analyzer. The average of 5–20 decays was generally sufficient to give an acceptable signal to noise ratio.

Gas mixtures were prepared by using a conventional vacuum line fitted with Teflon glass valves. Acetaldehyde (99%) from Fluka was carefully degassed. Ethylene (99.95%), propene (99%), isobutene (99%), 1-butene (99%), and 2-butene (99%) from l'Air Liquide were carefully degassed and used without further purification. Impurities are mainly other olefins which all have similar reactivities and alkanes which do not react with HCO.

Calculation Conditions. All molecular calculations were carried out within the framework of an ab initio formalism with double-ζ quality atomic basic sets in the valence region (3-21G).[6] Geometric structures were optimized at the SCF level, and a UHF[7] type of processing was applied to the radicals. Saddle points on the potential energy surface were obtained with a necessarily convergent algorithm[8] which ensured that the calculated saddle point would link the reactants with the products. These results were extended by evaluating force constant matrices for all geometry optimized transition states.

As a starting point to this study, we have undertaken preliminary calculations of the potential energy surface of the interacting constituents HCO and C_2H_4 in the context of the MNDO method[9] to locate the area of the stationary points. It appears that for the addition and hydrogen transfer reactions, the transition state occurs for a nonsymmetrical geometric structure, a reaction pathway without any particular symmetry being the most favorable. Thus 21 internal coordinates are required to describe the addition and hydrogen atom transfer mechanisms.

This ab initio study is complemented by a standard statistical mechanical treatment[10,11] in order to discuss the rate parameters for both reactions in comparison with the experimental data. All necessary quantities can in principle be obtained from the molecular surface under investigation. In our calculation of the vibrational partition function, the frequencies are taken from experiment or estimated data for several reactants and products and from calculations for the addition compound and transition states implicated in the two mechanisms. In such a case, a tunneling correction, the so called Wigner correction[12] is introduced. Although not well justified dynamically, the Wigner correction which was found to be generally important for hydrogen transfer, is a multiplicative factor which may be written as follows:

$$t = 1 + \frac{1}{24}\left(\frac{hc\,\bar{\nu}^{\ddagger}}{kT}\right)^2$$

where $\bar{\nu}^{\ddagger}$ is the modulus of the imaginary transition mode frequency in

(2) Lesclaux, R.; Veyret, B.; Roussel, P. *Ber. Bunsen-Ges. Phys. Chem.* **1985**, *89*, 330.
(3) Moortgat, G. K.; Slemr, F.; Seiler, W.; Warneck, P. *Chem. Phys. Lett.* **1978**, *54*, 444.
(4) Veyret, B.; Lesclaux, R. *J. Phys. Chem.* **1981**, *85*, 1918.
(5) Veyret, B.; Roussel, P.; Lesclaux, R. *Chem. Phys. Lett.* **1984**, *103*, 389.
(6) Ditchefield, R.; Hehre, W. J.; Pople, J. A. *J. Chem. Phys.* **1971**, *54*, 724.
(7) Csizmadia, I. G. *Progress in Theoretical Chemistry*; Elsevier: Amsterdam, 1976; Vol. 1.
(8) Liotard, D.; Penot, J. P. *Spring in Synergetics*; Della Dora, J.; Demongeot, J.; Lacolle, B. Springer: Berlin, 1981; Vol. 9, p 213.
(9) Dewar, M. J. S.; Thiel, W. *J. Am. Chem. Soc.* **1977**, *99*, 4899.
(10) Benson, S. W. *Thermochemical Kinetics*, 2nd Ed.; Wiley: New York, 1976.
(11) Davidson, N. *Statistical Mechanics*, McGray Hill, New York: 1982.
(12) Wigner, E. *Z. Phys. Chem., Abt B*, **1932**, *19*, 203.

cm^{-1}, h and k being respectively Planck's and Boltzmann's constants.

Results and Discussion

I. Experimental Study. Since acetaldehyde was photolyzed in a Pyrex cell there was no possibility of a direct photolysis of the olefins. The spectral distribution of the actinic light ranged roughly from 300 to 350 nm. In this region, acetaldehyde is principally photodissociated, into CH_3 and HCO. The other possible photodissociation channels yielding either CH_4 + CO or CH_3CO + H account for less than 5% of the total quantum yield.

All experiments were carried out by using an acetaldehyde concentration of 1.6×10^{18} molecule·cm^{-3} (50 torr at 298 K). The kinetics of the HCO reactions were measured for various olefin concentrations: $8–21 \times 10^{18}$ molecule·cm^{-3} (200–650 torr at 298 K). Higher concentrations could not be used, due to the high pressure that developed in the cell at high temperatures.

Considering that only CH_3 and HCO are produced in the photolysis of acetaldehyde, the following simplified reaction mechanism is expected to occur:

$$CH_3CHO + h\nu \rightarrow CH_3 + HCO$$

$$HCO + \text{olefin} \rightarrow \text{products (radical)} \quad (8)$$

$$CH_3 + \text{olefin} \rightarrow \text{products (radical)} \quad (9)$$

$$CH_3 + CH_3CHO \rightarrow CH_4 + CH_3CO \quad (10)$$

$$HCO + HCO \rightarrow CO + CH_2O \quad (11)$$

$$HCO + R \rightarrow CO + RH \quad (12)$$

$$R + R \rightarrow \text{products (molecules)} \quad (13)$$

where R represents all radicals present in the reacting system apart from HCO.

Acetaldehyde was chosen instead of formaldehyde as a source of HCO radical, to avoid secondary sources of HCO. Indeed, the photolysis of CH_2O yields H atoms which are rapidly converted into alkyl radicals in the presence of olefins. The alkyl radicals would then react by hydrogen abstraction from CH_2O, especially at high temperatures, producing more HCO radicals and thereby complicating the HCO decay kinetics. The possibility of a secondary formation of HCO with acetaldehyde is highly unlikely.

The absorption cross section of HCO at 614.5 nm is fairly low: 1.07×10^{-18} cm^2 and therefore the sensitivity of detection of the radical is rather poor. This is a source of difficulty in the measurements of rate constants of slow reactions such as those of HCO with olefins. The smallest measurable initial absorption of the HCO decay, corresponding to a reasonable signal to noise ratio when averaging 20 traces, was of the order of 2–3%. This corresponded to fairly high radical concentrations: 1×10^{13} molecule-cm^{-3} and consequently, radical recombination could not always be neglected, particularly at the lowest temperatures and olefin concentrations. The rate constants of reaction 8 therefore had to be derived from computer simulation of experimental decays, by using the above reaction mechanism.

The simulations were performed by adjusting the value of k_8 until a good fit between the calculated and experimental decay was obtained. The value of the rate constant for reaction 11 was taken from ref 5: 3.35×10^{-11} cm^3·molecule^{-1}·s^{-1}. For simplification, the rate constant value 3×10^{-11} cm^3·molecule^{-1}·s^{-1} was assigned to all other radical–radical reactions (reactions 12 and 13). Consequently, reactions 9 and 10 could be ignored since they do not correspond to any loss or production of radicals. Absolute radical concentrations were deduced from the initial HCO absorption, using the absorption cross section determined with the same experimental setup.[5] It should be pointed out, however, that in most cases and particularly at temperatures higher than 400–420 K the decays were very close to the pseudo-first-order conditions and could be analyzed as pure exponential curves. As a result, the uncertainties on measurements were the highest at the lowest temperatures. Measurements were no longer possible at temperature lower than 320–350 K, depending on the olefin concentration; i.e., rate constant values smaller than 3×10^{-17} cm^3·molecule^{-1}·s^{-1} could not be determined.

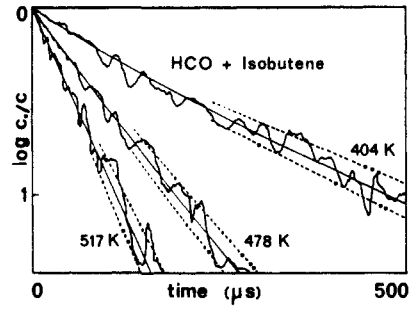

Figure 1. Example of a plot of the decay of HCO concentration vs. time on a logarithmic scale. The isobutene concentration is 1.62, 0.81, and 1.13×10^{19} molecule cm^{-3} at 404, 478, and 517 K, respectively. $C_0 = [HCO]_0$ is 1.3, 3.6, and 3.2×10^{13} molecule cm^{-3} at 404, 478, and 517 K, respectively. The solid lines are the best fit simulations. The dashed lines are simulations with a ±20% variation of the rate constant k_8.

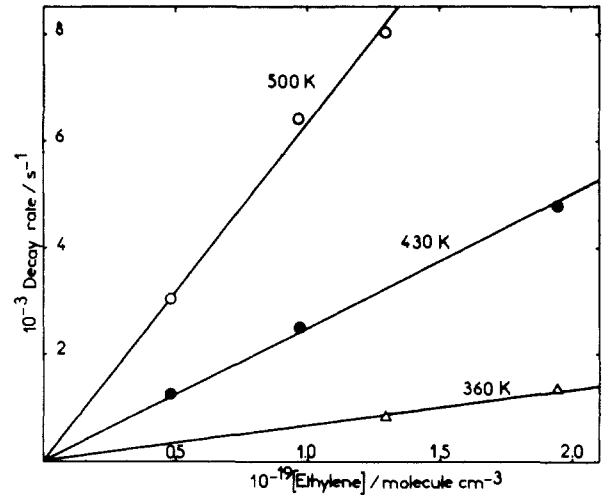

Figure 2. Plot of the pseudo-first-order decay rate of HCO against ethylene concentration. The acetaldehyde concentration was 1.6×10^{18} molecule·cm^{-3} and no diluent gas was added.

An example of kinetic data treatment is given in Figure 1 where the HCO decay is plotted vs. time along with the simulations. This figure clearly shows that only at the lowest temperature is the radical–radical contribution non-negligible.

The low sensitivity of the HCO detection and the reduced photodissociation quantum yield of acetaldehyde at high pressure, resulted in a new difficulty in recording the small absorption decays. This difficulty arose from the necessity of firing the flash lamps at a fairly high energy in order to produce sufficient radical concentration. The flash lamp discharge induced a perturbation in the decay, which had the shape of a long transient absorption and which could be accurately recorded by slightly detuning the dye laser from the HCO absorption band head. This perturbation was essentially due to mechanical vibrations of the optical system. It represented one third to one half of the total absorption signal from which it was subtracted. A good indication of the validity of such a procedure was provided by the fact that good exponential decays were obtained when pseudo-first-order conditions were fulfilled (see Figure 1).

An example of the plot of the pseudo-first-order decay rates of HCO (or $k_8 \times$ [olefin] when k_8 was directly derived from computer simulation of the decays) against the olefin concentration is given in Figure 2 for the particular case of ethylene and at different temperatures. A fairly good linearity can be observed, and the lines correctly go through the origin. This shows that indeed the HCO radical reacts with the olefin and that the experimental conditions were satisfactory. It also shows that radical–radical reactions were correctly taken into account in simulations, when necessary.

Figure 2 also shows that the rate constant is very sensitive to the temperature. Arrhenius plots are represented in Figures 3, 4, and 5 for ethylene, propylene, and isobutene, respectively. Each

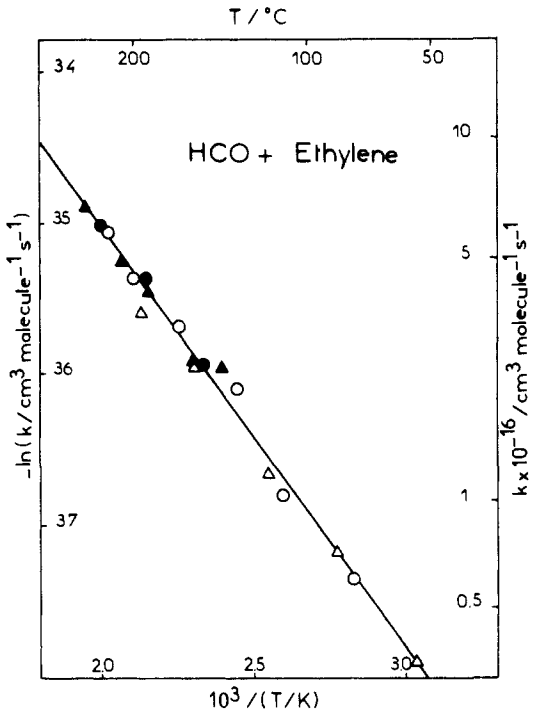

Figure 3. Arrhenius plot for the rate constant of the reaction of HCO with ethylene. Ethylene concentrations were the following (10^{18} molecule·cm^{-3}): ●: 4.9; ▲: 9.75; ○: 13.0; △: 19.5.

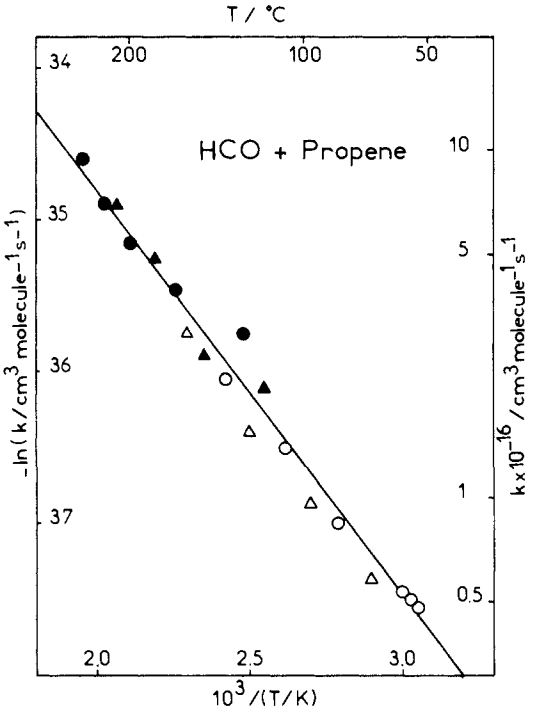

Figure 4. Arrhenius plot for the rate constant of the reaction of HCO with propene. Propene concentrations were the following (10^{18} molecule·cm^{-3}): ●: 9.1; ▲: 13.9; ○: 16.9; △: 20.5.

Table I. Experimental Arrhenius Parameters and Rate Constants at 298 and 450 K[b]

	10^{13}[a] A	E_a/kcal mol^{-1}	$10^{17}k_{298K}$[a]	$10^{16}k_{450K}$[a]
ethylene	1.5 ± 0.6	5.5 ± 0.15	1.5	3.3
propene	1.7 ± 0.9	5.4 ± 0.20	2.0	4.2
isobutene	5.45 ± 2.9	6.25 ± 0.26	1.5	5.25
1-butene	3.8 ± 2.7	6.0 ± 0.35	1.6	4.8
2-butene	3.3 ± 2.8	6.0 ± 0.44	1.4	4.2
1,3-butadiene	5.8 ± 1.3	4.1 ± 0.10	55	58

[a] cm^3·molecule^{-1}·s^{-1} units. [b] Uncertainties are equal to 2σ.

point represents an individual measurement, and the corresponding olefin concentration is indicated. This shows that plots similar to those shown in Figure 2 could be drawn for other compounds. Similar Arrhenius plots were obtained for the reaction of HCO with 1-butene and 2-butene, though a reduced number of experiments were performed in these cases, resulting in larger uncertainties in the results.

The Arrhenius parameters are reported in Table I for the five olefins studied and for butadiene.[2] The most striking feature is that the preexponential factors and activation energies are similar for all olefins: 2–6 × 10^{-13} cm^3·molecule^{-1}·s^{-1} and about 6 kcal·mol^{-1}, respectively. However, the difference observed between ethylene and the butenes appears to be significant, even though it is hardly larger than the combined uncertainties. A similar progression was observed in the Arrhenius parameters determined in a similar study of the NH_2 radical.[13] This is consistent with the fact that the same addition process to the double bond prevails for both radicals, as shown hereafter. The rate constants at 298 and 450 K are also included in Table I. The temperature of 450 K corresponds to the average of temperatures at which measurements were the most accurate. The reactions are very slow at room temperature, and the differences observed at 450 K, particularly for ethylene, propene, and isobutene, are significant, even though they are too small to be interpreted. As expected the rate of the reaction with butadiene is much faster than those with olefins, as the result of a smaller activation energy.

The uncertainties quoted in Table I correspond to two standard deviations. The principal cause of a possible systematic error would

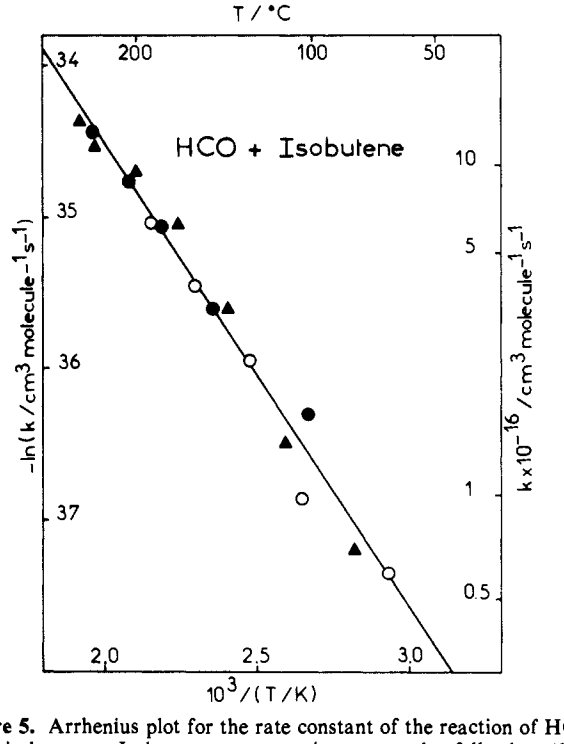

Figure 5. Arrhenius plot for the rate constant of the reaction of HCO with isobutene. Isobutene concentrations were the following (10^{18} molecule·cm^{-3}): ●: 8.1; ▲: 11.4; ○: 16.2.

be the presence of reactive impurities in olefins since high purity compounds could not be used due to the large amount of material required. However, impurities are essentially alkanes or other olefins, which have lower and similar reactivities, respectively, compared to the principal reactant.

Another indication of the absence of significant systematic errors is the expected value found for the preexponential factors. Indeed, preexponential factors corresponding to the addition to an olefinic double bond of radicals similar to HCO (3–4 atoms) are always in the same range of values. For example, the values range from 2 to 8 × 10^{-13} cm^3·molecule^{-1}·s^{-1} for the addition of NH_2 to the

(13) Khe, P. V.; Lesclaux, R. *J. Phys. Chem.* **1979**, *83*, 1119.

Table II. Compared Arrhenius Parameters and Rate Constants at 450 K for Reactions of HCO, CH_3, NH_2, and OH with Propene

	log $k_{450\,K}$[a]	log A[a]	E/kcal mol^{-1}	ref
HCO	−15.4	−12.8	5.4	this work
CH_3	−16.1	−12.2	7.4	10
NH_2	−14.4	−12.3	4.3	6
OH	−10.85	−11.4	(−1.1)	11

[a] k and A in cm^3·molecule^{-1}·s^{-1} units.

same olefins.[13] Similar values were also measured for methyl radicals.[14] The same remarks apply to the addition of these radicals to butadiene.[15,16] For example, a preexponential factor of 6.3×10^{-13} cm^3·molecule^{-1}·s^{-1} was found in the case of NH_2.[15]

It is of interest to compare the reactivity of HCO toward olefins to the corresponding reactivity of other radicals for which data are available. Since preexponential factors are generally close to each other, apart from OH reactions which exhibit A values higher by a factor of about 10, the reactivity is primarily determined by the activation energy. Arrhenius parameters are listed in Table II for the reactions of HCO, CH_3, NH_2, and OH with propene. Due to the high preexponential factor and the low activation energy, OH is the most reactive of these radicals. The reactivity of HCO is intermediate between those of NH_2 and CH_3. This is a fairly low reactivity, particularly at temperatures lower than 500 K. Consequently, it is unlikely that the reactions of HCO with unsaturated hydrocarbons play an important role in hydrocarbon oxidations, since either the fast reaction with molecular oxygen (reaction 1) or the decomposition at higher temperature (reaction 6) will always be predominant. However, they may be important in the temperature range of this study, in some particular photochemical systems involving aldehydes and olefins.

As usually observed for other radicals, the reaction of HCO with butadiene is faster than the reaction with olefins. This is essentially due to a lower activation energy for the addition to the conjugated diene: 4.15 kcal·mol^{-1} instead of about 6 kcal·mol^{-1} for the olefins. Similar progressions are observed for NH_2: 2.3[15] instead of about 4 kcal·mol^{-1} [13] and also for other radicals.[14,16]

As already pointed out, the rate constants and Arrhenius parameters do not vary significantly from one olefin to another. Therefore, the reactivity of HCO is not significantly sensitive to the degree of alkyl substitution of the double bond. This behavior, similar to that of NH_2 and CH_3, is indicative of the very small electrophilic character of HCO with respect to the olefins double bond attack. A larger increase of the addition rate constant, from ethylene to the butenes, would have been expected in case of a marked electrophilic character.

Determination of the Reaction Channel. It was shown above that two channels, the addition and the hydrogen atom transfer, are thermodynamically possible for the reaction of HCO with the olefinic double bond.

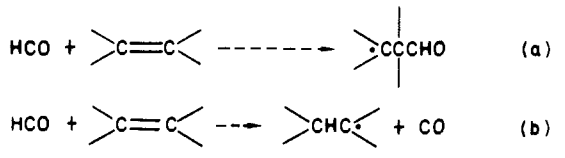

The reaction channel was determined in the particular case of isobutene by end product analysis in conventional photochemical experiments. They consisted of measuring the quantum yield of carbon monoxide since this product is only formed in channel b. Acetaldehyde (10 torr) was photolyzed at 313 nm and around 500 K in the presence of 200 torr of either isobutane or isobutene. Only a fraction of 10^{-4} of acetaldehyde was photolyzed, and the noncondensable gases at liquid nitrogen temperature, produced in the photolysis, were determined by using a mass spectrometric gas analyzer. The radical steady-state concentration was kept low, $<2 \times 10^{11}$ molecule·cm^{-3}, so that radical–molecule reactions were favored over radical–radical reactions.

In the presence of isobutane, the methyl radical generated in the photolysis of acetaldehyde at the same rate of HCO could only react with the alkane by hydrogen abstraction, producing therefore methane with a quantum yield close to one. This system was used as an actinometer.

In the presence of isobutene, the addition of HCO to the double bond forms a heavy radical which reacts by forming molecules condensable at liquid nitrogen temperature. Thus, the yield of CO, relative to that of CH_4 in the first experiment, gives directly the branching ratio for channels a and b.

Measurements gave $\phi_{CO} = 0.08 \pm 0.02$ for the quantum yield of CO. Considering that the molecular photodissociation of acetaldehyde at 313 nm

$$CH_3CHO + h\nu \rightarrow CH_4 + CO$$

accounts for about 5% of the CO yield and that traces of N_2 may have contributed to the small signal measured at $m/e = 28$, it can be concluded that channel b contributes less than 5% to the total reaction.

The addition process is therefore the principal, if not the only, reaction channel. The same conclusion was reached for the reaction of HCO with butadiene.[2]

Since the reaction is an addition process, a pressure dependence of the rate constant may be expected, particularly in the case of ethylene. However, high concentrations of olefins had to be used in this study, and it is likely that all experiments were carried out at the high pressure limit, as indicated by the linear plot in Figure 2. For NH_2, for example, only a small pressure effect could be detected at pressures lower than 5 torr.[13,18]

II. Theoretical Study. The theoretical ab initio SCF study concerns the reactants (C_2H_4 + HCO), the products (C_2H_5 + CO; C_2H_5CO), and the transition states implicated in the addition and hydrogen transfer reactions.

The stationary points of the potential energy hypersurface required by transition state theory were studied by using an ab initio method and paying particular attention to the activated complex.

The equilibrium configurations (Figure 6) of the ground states of reactants and products were located by using a quadratic interpolation optimization method.[19] The calculations on HCO, C_2H_4, CO, and C_2H_5 were therefore made taking symmetry into account. The configurations found are given in Table III. The optimized structures at the SCF level are in good agreement with previous experimental and theoretical data.[20-28] Concerning the addition compound C_2H_5CO, for which no experimental data exist, our calculations were done with no imposed symmetry and lead to the structural parameters shown in Table III.

Total and relative energies for reactants and products are also given in Table III. The exoenergicity of the hydrogen transfer and addition processes was determined by the difference between the energies of the (C_2H_4 + HCO) system in the reactant region (separation between the two fragments has been taken equal to 15 Å) and the product region of the potential energy surface. The calculated energy differences lead, for the two pathways, to exothermic reactions, and the most energetic one produces C_2H_5

(14) Cvetanovic, R. J.; Irvin, R. S. *J. Phys. Chem.* **1967**, *46*, 1964.
(15) Hack, W.; Schroter, M. R.; Wagner, H. Gg.; *Ber. Bunsen-Ges. Phys. Chem.* **1982**, *86*, 326.
(16) Abel, P. I., *Comprehensive Chemical Kinetics*; Bramford, C. H., Tipper, C. F. H. Eds.; Elsevier: Amsterdam, **1976**, *18*, 111.
(17) Atkinson, R.; Pitts, J. N., Jr. *J. Chem. Phys.* **1975**, *63*, 3591.
(18) Bosco, S. R.; Nava, D. F.; Brobst, W. D.; Stief, L. J. *J. Chem. Phys.* **1984**, *81*, 3505.
(19) Fletcher, R. *Comput. J.* **1970**, *13*, 317.
(20) Lathan, W. A.; Hehre, W. J.; Pople, J. A. *J. Am. Chem. Soc.* **1971**, *93*, 808.
(21) Pacansky, J.; Dupuy, M. *J. Chem. Phys.* **1978**, *68*, 4276.
(22) Pacansky, J.; Coufal, H. *J. Chem. Phys.* **1980**, *72*, 5285.
(23) Harding, L. B. *J. Am. Chem. Soc.* **1981**, *103*, 7469.
(24) Schlegel, H. B. *J. Phys. Chem.* **1982**, *86*, 4878.
(25) Delbecq, F.; Ilavsky, D.; Anh, N. T.; Lefour, J. M. *J. Am. Chem. Soc.* **1985**, *107*, 1623.
(26) Sorbie, K. S.; Murrel, J. N. *Mol. Phys.* **1975**, *29*, 1387.
(27) Dunning, T. H. *J. Chem. Phys.* **1980**, *73*, 2304.
(28) Geiger, L. C.; Schatz, G. C.; Harding, L. B. *Chem. Phys. Lett.* **1985**, *114*, 520.

Table III. 3-21G Optimized Structures (Distances in A, Angles in deg), Calculated Total Energies (hartrees), and Calculated Relative Energies (kcal·mol^{-1}) for Reactants, Products, and the Related Transition States

struct params	molecules						
	C_2H_4	HCO	TS_{add}	TS_{trans}	C_2H_5CO	C_2H_5	CO
R_1	1.315		1.381	1.381	1.512	1.507	
R_2			2.146		1.519		
R_2'				1.462		1.090	
R_3		1.181	1.195	1.157	1.208		1.129
r_1	1.074		1.077	1.085	1.072	1.074	
r_2	1.074		1.077	1.085	1.072	1.074	
r_3	1.074		1.080	1.100	1.085	1.084	
r_4	1.074		1.079	1.090	1.082	1.084	
r_5		1.093	1.089	1.285	1.086		
α_1	121.9		122.8	122.6	120.4	120.4	
α_2	121.9		122.8	122.6	120.4	120.4	
α_3	121.9		121.4	120.5	109.9	111.2	
α_4	121.9		121.1	118.1	109.2	111.2	
α_5		129.4	129.2	128.6	121.2		
β_1			104.0	106.9	111.4	111.2	
β_2				168.1			
β_3			118.4		124.7		
τ_1			87.8	80.0	89.8	83.8	
τ_2			90.3	96.7	90	83.8	
τ_3			99.9	100.5	120.8	119.7	
τ_4			102.2	116.6	119.4	119.7	
τ_5			82.2	83.7	87.6		
δ_1			79.0		90.4		
δ_2				0			
total energies	−77.60099	−112.60379	−190.19503	−190.17430	−190.24146	−78.16364	−112.09330
rel energies	0		6.1	19.1	−23.0	−32.7	

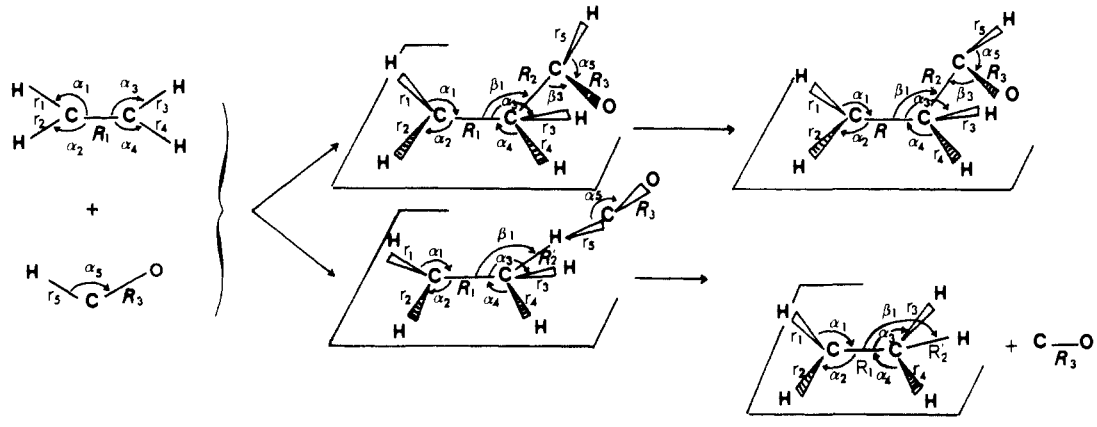

Figure 6. Coordinates for reactants, products, and related transition states (τ_n are dihedral between r_n and R_1R_2 or R_1R_2'; δ_1 and δ_2 are respectively dihedral between R_3 and R_1R_2 or $R_2'r_5$).

and CO. These results are in reasonable agreement with the thermodynamic data estimated from Benson's rules[10] and confirm that the ab initio UHF procedure corresponds to a good asymptotic behavior. It correctly reflects the energy of the fragments and enables one to take into account satisfactorily the supersystem in a bound state. For reactants and products, the $\langle S^2 \rangle$ value obtained from the UHF wave function is very close to the value of a pure doublet.

Transitions States. The SCF transitions states were located by using an algorithm developed in our laboratory.[8] This algorithm based on a digital processing of the energy relaxation is supported by the following mathematical property: the shifting along the gradient vector field of an arbitrary continuous path joining the reactants and the products leads to a limiting path whose highest energetic point is a saddle point. For the hydrogen transfer and addition processes the calculations were done with unconstrained C_1 symmetry. In both cases the transition state force constants were determined from the analytic forces. The diagonalization of the 21 × 21 force constants matrix leads to eigenvalues and eigenvectors for the stationary points. As discussed by Murrell and Laidler[29] a true transition state will have a single imaginary vibrational frequency at the saddle point. Due to the extreme flatness of the potential hypersurface along the dihedral coordinates δ_1 and δ_2 for addition and hydrogen transfer, respectively, it is also interesting to note that the exceptionally small magnitude of the real frequencies characteristics of the torsional modes explains the difficulty in locating the saddle points.

The two structures of the unconstrained transition states for the addition and hydrogen transfer processes depicted in Figure 6 are also given in Table III.

It is fruitful to compare the stationary saddle point structures in Table III with the analogous equilibrium geometry of the reactants and products obtained in the two exit channels. Concerning the addition mechanism, the C–C single bond distance in C_2H_5CO (R_2 = 1.519 Å) is increased by 41% to 2.146 Å (ΔR_2 = 0.627 Å) for the addition transition state TS_{add}). A somewhat smaller fractional bond distance (~9%) is predicted for the other C–C distance (R_1) which is 1.512 Å for the adduct compound and 1.381 Å (ΔR_1 = −0.131 Å) for the TS_{add}. In this latter case this R_1 bond distance in TS_{add} is nearly the same as the corresponding ethylene value. At the same time, the CH distances and the typical angles about sp^2 hybridized carbon in ethylene are geometrically deformed to lead to an addition product involving two typical sp_2 and sp_3 hybridized carbons. For the HCO skeleton

(29) Murrell, J. N.; Laidler, K. J. *Trans. Faraday Soc.* **1968**, *64*, 371.

Table IV. Mulliken Population Analyses for Reactants, Products, and Transition States

	C_2H_4	HCO	TS_{add}	TS_{trans}	C_2H_5CO	C_2H_5	CO
R_1	0.531		0.382	0.349	0.232	0.249	
R_2			0.042		0.153		
R'_2				0.042		0.370	
R_3		0.441	0.455	0.457	0.519		0.441
r_1	0.395		0.387	0.387	0.381	0.381	
r_2	0.395		0.387	0.388	0.383	0.381	
r_3	0.395		0.381	0.382	0.354	0.378	
r_4	0.395		0.383	0.384	0.366	0.378	
r_5		0.236	0.243	0.050	0.350		

the TS_{add} structure is intermediate between reactants and the addition compound. As expected for exothermic reactions, it should be emphasized that the TS_{add} structure is intermediate between reactants and addition compounds and that the TS_{add} barrier is located well into the entrance channel. The reaction coordinate ($\bar{\nu}_{add}^{\ddagger}$ = 430 i cm^{-1}), primarily involving the R_2 valence bond joining the fragments but also implying a small contribution of the torsional δ_1 and τ_5 modes, gives the least energetic pathway on the saddle point. The computed SCF barrier height is found to be 6.1 kcal·mol^{-1}. However, comparison with the experimental activation energy requires at least that zero point energies, enthalpic and entropic terms, be taken into account.

For the hydrogen transfer mechanism, the computed saddle point depicted in Figure 6 is also given in Table III. It is of interest to note that the transition state for hydrogen transfer (TS_{trans}) lies also in this case closer to reactants (C_2H_4 + HCO) than to products (C_2H_5 + CO) verifying Hammond's postulate[30] which states that for an exothermic reaction, the transition state should resemble the reactant geometry. The CH bond r_5 from HCO is stretched by about 0.2 Å, and the CH distance R'_2 going to products is about 0.4 Å longer than the value for the CH bond on the typical sp^3 hybridized carbon for C_2H_5. There are some significant geometrical changes in the ethylene fragment, particularly an extension of the C–C bond (ΔR_1 = +0.066 Å), and a weak loss of sp^2 hybridization. Furthermore, at the transition state (TS_{trans}), the potential surface is fairly flat with respect to dihedral angles between the two fragments. The transition vector ($\bar{\nu}_{trans}^{\ddagger}$ = 1943 i cm^{-1}) is dominated by a CH asymmetric stretch (0.67 R'_2–0.67r_5) between the coordinate joining the reactants with small contributions coming from initial ethylenic R_1 and the dihedral angles between the attacking formyl and ethylenic carbon atoms. The low value of the imaginary frequency relative to a typical stretching ν_{CH} mode is due to the long (relative to normal chemical bonds) CH distance at the saddle point.

The calculated hydrogen transfer barrier of 19.1 kcal·mol^{-1} is much higher than that of the addition reaction (6.1 kcal·mol^{-1}). Although the hydrogen transfer reaction seems energetically more favorable than the addition mechanism, in view of the calculated enthalpy difference, it appears from the study of the potential hypersurface that the addition reaction should be kinetically more favorable and faster than hydrogen transfer as in the experiments.

The Mulliken population analyses are given in Table IV. The two processes can be described as involving in the first stage a very small electrophilic transfer of attacking hydrogen or carbon of formyl to carbon of C_2H_4: this is consistent with experimental observations. As expected there is a large decrease in the overlap population between "ethylenic carbon atoms".

It is noteworthy that at the transition state TS_{add} there is only a weak new bond R_2 between the attacking carbon and its nearest ethylenic carbon atom. The same situation is observed for TS_{trans} with the cleavage of the CH bond and the formation of ethyl radical. This suggests that the transition states are rather "early and slightly bonded" in spite of a weakening of the double bond and a loss of planarity in the alkene. For addition this would be consistent with the observations of Safarik and Strausz[31] and the results of Tedder and Walton[32] concerning the addition of alkyl and haloalkyl radicals to ethylene.

The inspection of $\langle S^2 \rangle$ shows that in all transition states the rather large values obtained from the UHF wave function (S^2 = 1.04) of an impure spin state are not close to the value of a pure doublet.

Table V. Calculated Thermodynamic[a] Values for Addition and Hydrogen Transfer Processes at 298 K

	addition	H atom transfer
ΔE_{UHF}	−23.0	−32.7
$\Delta H_0°$	−20.75	−32.2
$\Delta(h_{298}° - h_0°)$	−1.35	−0.03
$\Delta H_{298}°$	−22.1	−32.2
$\Delta S_{298}°$	−39.0	−2.4
$\Delta G_{298}°$	−10.5	−31.5

[a] Standard enthalpies $\Delta H_{298}°$ in kcal·mol^{-1}. Standard entropies $\Delta S_{298}°$ in cal·mol^{-1}·K^{-1}. Standard free energies $\Delta G_{298}°$ in kcal·mol^{-1}.

Table VI. Calculated Arrhenius Parameters for Addition and Hydrogen Atom Transfer Mechanisms between 298 and 513 K

	addition		H atom transfer	
T (K)	E_a (kcal·mol^{-1})	A[a]	E_a (kcal·mol^{-1})	A[a]
298	6.9	1.56×10^{-13}	20.3	2.64×10^{-13}
373	7.1	2.35×10^{-13}	20.5	3.99×10^{-13}
448	7.6	3.52×10^{-13}	20.9	6.04×10^{-13}
513	7.8	4.90×10^{-13}	21.1	8.41×10^{-13}
av[b]	7.2	2.55×10^{-13}	21.0	6.1×10^{-13}

[a] cm^3·molecule^{-1}·s^{-1}. [b] From the Arrhenius plot of the calculated rate constants for each temperature.

Thermodynamic Study. The thermodynamic study takes into account the correction arising from the vibrational zero point energy (ΔZPE) as well as the influence of the enthalpic and entropic terms. Using UHF energies has enabled us to gain insight into the enthalpies $\Delta H_T°$ and free energies $\Delta G_T°$ of the addition and hydrogen transfer reactions. $\Delta H_T°$ is subsequently determined as a function of $\Delta E_{UHF}°$, ΔZPE, and of the enthalpy terms $\Sigma_i \nu_i (h_T° - h_0°)_{A_i}$ calculated for each of the two reaction channels, by using the partition functions deduced from structural and spectroscopic values of reactants and products from our calculations (Table V).

$$\Delta H_T° = \Delta E°_{UHF} + \Delta ZPE + \sum_i \nu_i (h_0^T - h_0°)_{A_i}$$

$$\Delta G_T° = \Delta H_T° - T\Delta S_T°$$

It is to be noted that the electronic contribution to these enthalpic and entropic terms for reactants and products has been neglected.

As shown by our calculations, the relative exothermicity of the hydrogen transfer products in comparison to the addition compound is slightly modified by considering the zero point vibrational correction. For addition the value $\Delta H_{298}°$ = −22.1 kcal·mol^{-1} is in agreement with the estimation from thermochemical data[10] while the calculation value for hydrogen transfer $\Delta H_{298}°$ = −32.2 kcal·mol^{-1} is probably overestimated. The value of the entropy terms are very different for the two processes, and it is necessary to notice the importance of $\Delta S°$ for addition ($\Delta S_{298}°$ = −39 cal·mol^{-1}·K^{-1}). It thus becomes clear that the contribution of the entropy term is considerable for addition ($-T\Delta S_{298}°$ = 11.6 kcal·mol^{-1}), strongly shifting the thermal equilibrium toward the

(30) Hammond, J. S. *J. Am. Chem. Soc.* **1955**, *77*, 334.
(31) Safarik, I.; Strausz, O. P. *J. Phys. Chem.* **1972**, *76*, 3613.
(32) Tedder, J. M.; Walton, J. C. *Acc. Chem. Res.* **1976**, *9*, 183.

reactants C_2H_4 and HCO when the temperature increases.

Kinetic Study. The kinetic aspects of these addition and hydrogen transfer reactions (Tables V and VI) are examined and developed in the context of the TST method[33] for comparison to the experimental results.

The energy difference $\Delta E^{\ddagger}_{UHF}$ between reactants and transition states is not directly comparable to the activation energy E_a described by the TST method.

$$E_a = nRT + \Delta H_T^{\circ\ddagger}$$

In this expression n is the molecularity and $\Delta H_T^{\circ\ddagger}$ the standard enthalpy change of the reaction considered: either HCO + C_2H_4 $\rightleftharpoons$ TS_{add} or HCO + C_2H_4 $\rightleftharpoons$ TS_{trans}.

For these reactions the standard enthalpy $\Delta H_T^{\circ\ddagger}$ is

$$\Delta H_T^{\circ\ddagger} = \Delta E^{\ddagger}_{UHF} + \sum_{i=1}^{3N-7} \tfrac{1}{2}hc\bar{\nu}_i(TS) - \sum_{\text{reactants}}\{\sum_{i=1}^{3N-6} \tfrac{1}{2}hc\bar{\nu}_i\} + \sum_i \nu_i(h_T^{\circ} - h_0^{\circ})_{A_i}$$

where the enthalpic terms $(h_T^{\circ} - h_0^{\circ})_{A_i}$ corresponding to constituents A_i can be evaluated from partition functions. $\Delta H_T^{\circ\ddagger}$ will subsequently be represented as

$$\Delta H_T^{\circ\ddagger} = \Delta E^{\ddagger}_{UHF} + \Delta$$

Under these conditions, the activation energy $E_a = \Delta E^{\ddagger}_{UHF} + \Delta + nRT$ calculated at any temperature differs from the theoretical calculation by the quantity $\Delta + nRT$. This corrective term, evaluated as 0.8 kcal·mol^{-1} for addition and 1.2 kcal·mol^{-1} for hydrogen transfer at 298 K, increases rapidly with temperature reaching respectively 1.7 kcal·mol^{-1} and 3 kcal·mol^{-1} at 513 K. For the temperature range of 298–513 K, the contribution of the corrective term is important and increases respectively by 10% to 22% and 6% to 15% the addition and hydrogen transfer barrier heights calculated within the UHF procedure. Thus, the activation energies become 6.9 kcal·mol^{-1} (addition) and 20.3 kcal·mol^{-1} (H transfer) at 298 K and are increased to 7.8 kcal·mol^{-1} and 22.1 kcal·mol^{-1}, respectively, at 513 K.

The analogous values of the preexponential factor A over the temperature ranges 298–513 K are calculated to be 1.56×10^{-13} to 4.90×10^{-13} cm^3·molecule^{-1}·s^{-1} for addition and 2.64×10^{-13} to 8.41×10^{-13} cm^3·molecule^{-1}·s^{-1} for hydrogen transfer. These values agree with the experimental results because the absolute entropy of activation obtained from ab initio calculations is generally close to the corresponding experimental values. Indeed entropies are reproduced well partly because double-ζ basis set calculations often give optimized geometries of very good quality: molecular structure is directly involved in the rotational partition function which is usually orders of magnitude larger than the thermodynamic vibrational function.

The correction for the tunneling effect, calculated with the Wigner formalism,[12] resulted in minor changes. It was found to be more important for the hydrogen transfer activation energy (−1 kcal·mol^{-1}) than for addition (−0.2 kcal·mol^{-1}). The preexponential factor also decreases over the temperature range examined.

In the light of this kinetic study it is possible to conclude that the addition channel is the main, if not the only, reaction channel corroborating the experimental conclusions. In addition, this study shows that the hydrogen atom transfer channel has a much higher activation energy and should not be efficient, even at higher temperatures than those of the present experimental and theoretical study.

By restricting ourselves to the HF approximation we have implicity omitted the effects of electron correlation and a more exact treatment based on the CI method with the same basis set would be worthwhile. Nevertheless, the results and trends found here are expected to retain their essential validity in the kinetic study. Indeed, since TS_{add} and TS_{trans} resemble the reactants and are rather "early", we can believe that the correlation corrections in the activation energy calculations should be small.

Conclusion

The present experimental and theoretical study provides new information on the reactivity of the HCO radical with unsaturated hydrocarbons and on the mechanism of the reactions. Both experimental end-product analysis and quantum mechanical calculations of the potential energy surfaces involved in the two possible reaction pathways clearly show that the HCO radical adds to the unsaturated bonds of olefins or butadiene. This is the first characterized reaction of HCO in which there is no hydrogen atom transfer from the weak CH bond of the radical. It is interesting to point out that the kinetic parameters determined either experimentally or theoretically are in reasonable agreement.

The reactivity of HCO is very similar for all the olefins of the series that we have studied, indicating that the same addition mechanism prevails in all cases. This is also indicative of the low electrophilic character of HCO in these reactions, which is corroborated by the Mulliken population analysis. Such a behavior is similar to that of the alkyl and NH_2 radicals for which similar detailed kinetic data are available.

As already pointed out, the reactions studied in this work are potentially important in hydrocarbon oxidation processes even though they have not been considered so far. Our results show, however, that the reactivity of HCO with respect to olefins is actually low and that these reactions are likely to be minor relative to the reaction of HCO with oxygen or its decomposition (reactions 1 and 6). This is also true in photochemical studies of aldehydes at low temperature, in which olefins have been used as hydrogen atom scavengers. The reaction is too slow, ($k_{298K} \approx 1.5 \times 10^{-17}$ cm^3·molecule^{-1}·s^{-1}) to compete with the reactions with O_2, NO, or other radicals in the absence of O_2 and NO. The reaction of HCO with butadiene however is significantly faster than the reaction with olefins and may be important under some particular conditions.

Acknowledgment. Calculations have been carried out on the CRAY-1 computer of the C.C.V.R. We thank the scientific council of the C.C.V.R. for the receipt of the computing grant.

Registry No. Formyl radical, 2597-44-6; ethylene, 74-85-1; propene, 115-07-1; isobutene, 115-11-7; 1-butene, 106-98-9; 2-butene, 107-01-7; butadiene, 106-99-0.

(33) Johnston, H. S. *Gas Phase Reaction Rate Theory*; Ronald Press: New York; 1966.